IR Band Profiling of Dichlorodifluoromethane in the Greenhouse Window: High-Resolution FTIR Spectroscopy of ν_2 and ν_8

Corey J. Evans,[†] Atilla Sinik,[‡] Chris Medcraft,[§,⊥] Don McNaughton,[§] Dominique Appadoo,[∥] and Evan G. Robertson*,[‡]

[†]Department of Chemistry, University of Leicester, University Road, Leicester LE1 7RH, U.K.
[‡]Department of Chemistry & La Trobe Institute of Molecular Sciences, La Trobe University, Victoria 3086, Australia
[§]School of Chemistry, Monash University, Victoria 3800 Australia
[∥]Australian Synchrotron, 800 Blackburn Road, Clayton, Victoria 3168, Australia

S *Supporting Information*

ABSTRACT: The IR spectrum of dichlorodifluoromethane (i.e., R12 or Freon-12) is central to its role as a major greenhouse contributor. In this study, high-resolution (0.000 96 cm^{-1}) Fourier transform infrared spectra have been measured for R12 samples either cooled to around 150 K or at ambient temperature using facilities on the infrared beamline of the Australian Synchrotron. Over 14 000 lines of $C^{35}Cl_2F_2$ and $C^{35}Cl^{37}ClF_2$ were assigned to the b-type ν_2 band centered around 668 cm^{-1}. For the c-type ν_8 band at 1161 cm^{-1}, over 10 000 lines were assigned to the two isotopologues. Rovibrational fits resulted in upper state constants for all these band systems. Localized avoided crossings in the ν_8 system of $C^{35}Cl_2F_2$, resulting from both a direct b-axis Coriolis interaction with $\nu_3 + \nu_4 + \nu_7$ and an indirect interaction with $\nu_3 + \nu_4 + \nu_9$, were treated. An improved set of ground state constants for $C^{35}Cl^{37}ClF_2$ was obtained by a combined fit of IR ground state combination differences and previously published millimeter wave lines. Together these new sets of constants allow for accurate prediction of these bands and direct comparison with satellite data to enable accurate quantification.
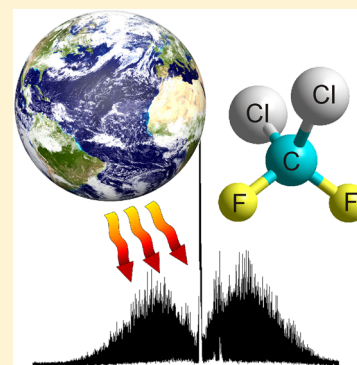
INTRODUCTION

R12 (also known as Freon-12), or CCl$_2$F$_2$, is a colorless gas that in the past was used as refrigerator and propellant gas. With the introduction of the Montreal Protocol the manufacture of R12 was banned in many countries as there was evidence that it was causing serious damage to the ozone layer. R12 is relatively stable in the atmosphere and has a long lifetime in the troposphere; however, in the stratosphere it undergoes photolysis by solar UV radiation, releasing chlorine atoms capable of catalyzing the breakdown of ozone. R12 is estimated to account for over 40% of the ozone depletion. It is also a major greenhouse gas, with a 100 year Global Warming Potential of 10 900[1] and a radiative forcing contribution exceeded only by carbon dioxide (CO$_2$), methane (CH$_4$), and very recently nitrous oxide (N$_2$O).[2] This is due in part to the coincidence of its strongest IR fundamentals with the atmospheric IR window (800−1400 cm^{-1}).[3] The atmospheric significance of R12 has spurred measurement of its concentrations, with the average global concentration being 270 ppt in 1978, rising to 544 ppt from 2001 to 2003 before falling to 530 ppt in early 2011.[4,5] Although the concentration of R12 is falling, its long tropospheric lifetime of ≈100 years means its greenhouse and ozone depleting effects on the Earth's climate will be felt for some time.

The monitoring of molecules like R12 in the atmosphere is extremely important. In the past, high-resolution infrared spectroscopy was extremely useful in analyzing atmospheric species and determining their concentration in the atmosphere. Some of its usefulness has been overtaken by other techniques, such as GC and GC/MS based methods. However, with more spectrometer-based satellite systems being used for monitoring molecular species, such as R12, in the atmosphere the demand for accurate spectroscopic data on these molecular species is now again on the increase. It has been shown that "only laboratory parameters measured at high resolution reproduce the satellite observations well."[6] As a result of this it is mandatory that accurate spectroscopic constants for these compounds are available.

For R12, several microwave and millimeter wave studies have been carried out, resulting in accurately known ground state constants for the two most abundant isotopic forms $C^{35}Cl_2F_2$ and $C^{35}Cl^{37}ClF_2$.[7−11] A set of constants for the $C^{37}Cl_2F_2$ isotopologue was obtained via IR-MW double resonance experiments.[12] The only other isotopologue studied has been $^{13}C^{35}Cl_2F_2$ by Takeo and Matsumura in addition to Davis et al.[8,9] The $C^{35}Cl_2F_2$, $C^{35}Cl^{37}ClF_2$, and $C^{37}Cl_2F_2$ isotopologues occur in the approximate ratio 9:6:1. $C^{35}Cl^{37}ClF_2$ has C_s

symmetry whereas $C^{35}Cl_2F_2$ and $C^{37}Cl_2F_2$ both have C_{2v} symmetry.

Evaluation of the force field of R12 has been performed by Giorgianni et al. and Davis et al. on the basis of low-resolution infrared spectra.[8,15] Table 1 outlines the wavenumber values

Table 1. Overview of Observed Fundamental Bands of CCl_2F_2 (All Values in cm^{-1})

mode	symmetry	$C^{35}Cl_2F_2$	$C^{35}Cl^{37}ClF_2$[a]	reference
ν_1	A_1	1101.3763		21
ν_2	A_1	668.4456	667.2074	this work
ν_3	A_1	458.6	455.7	13,14[b]
ν_4	A_1	261.6	259.1	15
ν_5	A_2	320.7	319.5	15
ν_6	B_1	923.2396	921.8192	17,18
ν_7	B_1	437.7		13, 14[b]
ν_8	B_2	1161.0851	1160.9649	this work
ν_9	B_2	437.0		13, 14[b]

[a]$C^{35}Cl^{37}ClF_2$ has C_s symmetry: $A' = A_1 + B_1$; $A'' = A_2 + B_2$.
[b]Reassessment of ν_3, ν_7, and ν_9 values based on solid state IR and Raman data of LeBlanc et al.,[13] and on MP2/aug-cc-PVTZ anharmonic frequency calculations and high-resolution band assignments for $\nu_2 + \nu_3$, $\nu_2 + \nu_7$, and $\nu_2 + \nu_9$ along with the far IR spectrum of R12 at 155 K.[14]

and symmetry of the vibrational bands of both $C^{35}Cl_2F_2$ and $C^{35}Cl^{37}ClF_2$ that have been examined to date. The ν_3, ν_7, and ν_9 fundamentals in the 400−500 cm^{-1} region are reassessed in light of solid state IR and Raman spectra measured by LeBlanc and Anderson,[13] and of high-resolution analysis of the ν_1, $\nu_3 + 2\nu_5$, $\nu_2 + \nu_3$, $\nu_2 + \nu_7$, and $\nu_2 + \nu_9$ region around 1100 cm^{-1} supported by MP2/aug-cc-PVTZ anharmonic frequency calculations.[14] It can be seen that only a few bands have been studied using high-resolution techniques, whereas the remainder have been studied using medium to low resolution. In the first high-resolution infrared investigation of R12, carried out by Nordstrom et al. in 1979, the ν_6 antisymmetric CCl_2 stretch band of $C^{35}Cl_2F_2$ around 923 cm^{-1} was studied using a diode laser and a FTIR spectrometer.[16] Jones and Morillon-Chapey carried out infrared-microwave double resonance spectroscopy on the ν_6 band of $C^{35}Cl_2F_2$,[17] followed a few years later by similar studies on $C^{35}Cl^{37}ClF_2$[18] and on $C^{37}Cl_2F_2$ and hot-bands of $C^{35}Cl_2F_2$ and $C^{35}Cl^{37}ClF_2$.[12] In 1988, Snels and Meerts re-examined the ν_6 band of $C^{35}Cl_2F_2$ and of $C^{35}Cl^{37}ClF_2$ in a molecular beam using a diode laser.[19] Giorgianni et al. investigated the band around 1101 cm^1 at high resolution (0.002 cm^1) and at a temperature of 200 K. In this study they obtained rovibrational assignments for the ν_1 fundamental, the symmetric CF_2 stretch, of $C^{35}Cl_2F_2$.[20] The upper state showed evidence of Coriolis resonance perturbations, and a fit could be obtained only by removing the most heavily perturbed transitions. McNaughton et al. completed two high-resolution studies on the ν_1 and ν_8 bands using a FTIR spectrometer coupled to a supersonic jet expansion chamber to measure spectra at a rotational temperature of 40 K.[21,22] For ν_8, the antisymmetric CF_2 stretch around 1161 cm^{-1}, upper state constants were obtained for $C^{35}Cl_2F_2$ and $C^{35}Cl^{37}ClF_2$ isotopologues. In the ν_1 work, a set of low-J transitions of $C^{35}Cl_2F_2$ were assigned and fitted, but the resultant constants were unable to adequately simulate the more perturbed transitions with J' up to 46 found by Giorgianni et al.,[20] nor those of even higher J revealed most recently by preliminary

analysis of the room temperature spectra.[23] D'Amico et al. studied the Fermi-resonance enhanced $\nu_3 + \nu_7$ combination band of $C^{35}Cl_2F_2$ and $C^{35}Cl^{37}ClF_2$ using high-resolution diode laser and FTIR supersonic jet techniques,[24] while also pointing to the need for further analysis of the polyad bands in the region 1000 ± 200 cm^{-1}.

In this present work we have obtained high-resolution (0.000 96 cm^{-1}) FTIR spectra of CCl_2F_2 at ambient temperature, and cooled to around 150 K. We report the first rovibrational analysis of the fourth most intense fundamental and the last stretching mode to be studied, the CCl_2 symmetric stretch ν_2 (668.5 cm^{-1}) for both $C^{35}Cl_2F_2$ and $C^{35}Cl^{37}ClF_2$. Re-examination of the ν_8 (1161 cm^{-1}) band in the greenhouse window yields much improved rovibrational constants and reveals localized Coriolis-induced perturbations in $C^{35}Cl_2F_2$ that have much less effect in $C^{35}Cl^{37}ClF_2$. Identification of the perturbing states supports reassignment of some of the fundamental vibrations of this molecule.

EXPERIMENTAL METHOD

The spectra of the ν_2 and ν_8 bands of R12 were recorded at maximum resolution (nominally 0.000 96 cm^{-1}) on the high-resolution infrared beamline of the Australian Synchrotron. The synchrotron provides a continuous source that is brighter than thermal sources offering a significant signal-to-noise advantage for high-spectral-resolution measurements (where restricted apertures are required) and particularly in the far IR region.[25,26] The experimental method and the design of the collisional cooling cell have been outlined previously.[27] In brief, the collisional cooling cell, set to a 2.5 m optical path length, was fitted with KBr windows and coupled to a Bruker IFS125HR spectrometer equipped with a KBr beamsplitter and either an external SiB helium cooled detector (for the far IR region containing ν_2) or a mercury−cadmium−telluride detector (for the mid-IR region containing ν_8). The ν_2 spectrum was measured with the temperature ranging between 153 and 159 K, with a sample pressure of R12 (Sigma-Aldrich >99%) maintained at 66−80 Pa, and by coadding 703 scans. In the ν_8 region, a total of 166 scans were collected at sample pressures of 2.0, 2.8, or 6.0 Pa and temperature 142−153 K. Also in this region, room temperature spectra totalling 768 scans were measured using 4.4 Pa of R12 in a standard White cell (Infrared Associates) with path length set to 6.6 m. The final spectra were calibrated against residual CO_2 lines in the far IR region and N_2O in the mid-IR region to within 0.0006 cm^{-1}.

RESULTS AND DISCUSSION

Analysis of ν_2. In the initial analysis of the ν_2 band the spectral analysis program MacLoomis was used to help in the assignment of the spectral lines by the vertical stacking of lines with the same K_a and K_c values.[28] Once the initial assignment was made, the program PGopher[29] and finally SPFIT[30] was used for the remainder of the analysis for both spectral assignment and line fitting. Figure 1 shows the spectrum of the b-type band of ν_2.

A total of 14 596 lines were assigned between 649.0 and 686.8 cm^{-1} to $C^{35}Cl_2F_2$ and $C^{35}Cl^{37}ClF_2$. No lines were assigned to the $C^{37}Cl_2F_2$ isotopologue. R12 is a prolate symmetric top molecule with an asymmetry parameter (κ) of −0.570. As previously mentioned, $C^{35}Cl_2F_2$ has C_{2v} symmetry and the ν_2 CCl_2 symmetric stretching mode has A_1 symmetry resulting in a b-type band. The symmetry of $C^{35}Cl^{37}ClF_2$ is C_s

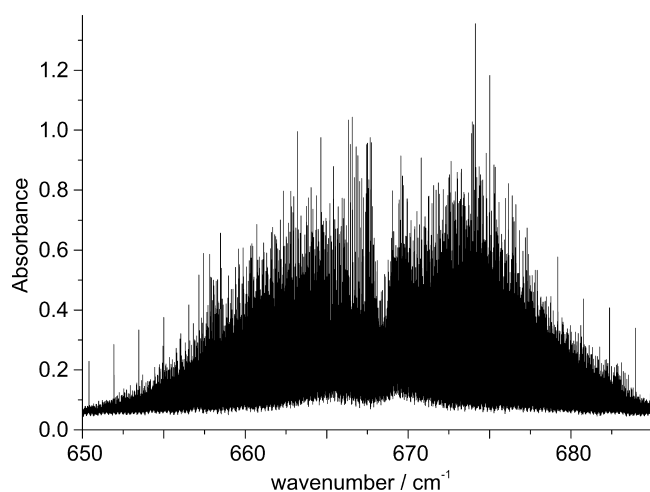**Figure 1.** b-type band ν_2 from the CF_2 deformation mode of CCl_2F_2.

and so the ν_2 band for this isotopologue has A′ symmetry implying an a/b-type band, but it is predominantly b-type in nature, i.e., $\Delta K_a = \pm 1$, $\Delta K_c = \pm 1$.

For the analysis of the $C^{35}Cl_2F_2$ species the ground state constants were fixed to those obtained by Baskakov et al.[11] For the $C^{35}Cl^{37}ClF_2$ isotopologue, the best ground state constants available in the literature are those of Booker and De Lucia,[7] with centrifugal distortion constants extending only to quartic level and based on rotational transitions with $J_{max} = 56$ and $K_{a\ max} = 31$. When these constants were used to predict ground state combination differences for comparison with an experimental set derived from our ν_2 and ν_8 data sets, small but systematic discrepancies (<0.001 cm^{-1}) were found for some transitions with quantum numbers up to $J = 81$ and $K_a = 65$. To improve the ground state constants for $C^{35}Cl^{37}ClF_2$, a combined fit was performed involving 87 rotational transitions from Davis and Gerry,[8] and from Booker and De Lucia,[7] together with 3007 ground state combination differences from both ν_2 and ν_8 data sets. The sextic centrifugal distortion constants were fixed to those of the $C^{35}Cl_2F_2$ species,[8] whereas the rotational and quartic centrifugal distortion constants were freely varied. Watson's A-reduced Hamiltonian was employed throughout using the I^r representation.[31]

Tables 2 and 3 show the fitted constants from the analysis of $C^{35}Cl_2F_2$ and $C^{35}Cl^{37}ClF_2$. In total, 13 upper state parameters were varied to fit the 8739 observed ν_2 transitions of $C^{35}Cl_2F_2$, whereas 11 parameters were fitted to the 5857 ν_2 transitions of $C^{35}Cl^{37}ClF_2$, with each line given a nominal standard deviation of 0.0002 cm^{-1}. The resulting root mean square (rms) error of 0.000 09 cm^{-1} for both $C^{35}Cl_2F_2$ and $C^{35}Cl^{37}ClF_2$ indicates an excellent fit. The analysis of both isotopologues indicates that there is no observable perturbation of the band from resonances with nearby fundamental, combination, or overtone modes. Figure 2 shows a small portion of the observed spectrum with the simulated combined spectra of $C^{35}Cl_2F_2$ and $C^{35}Cl^{37}ClF_2$ overlaid. It is clearly seen that the derived molecular parameters can model both the observed line positions and their intensities well.

Analysis of ν_8 $C^{35}Cl_2F_2$. Beginning with the constants derived from the jet-cooled spectra,[22] it was possible to assign over 6000 c-type transitions of ν_8, the antisymmetric CF_2 stretch, for the $C^{35}Cl_2F_2$ isotopologue. Most of the transitions were obtained from the better resolved 150 K spectrum, but the line list was supplemented by some high rotational quantum

Table 2. Spectroscopic Constants of the Fundamental Band ν_2 of $C^{35}Cl_2F_2$

parameter	ground state[a]	$\nu_2 = 1$[b]
ν_0 (cm^{-1})		668.4456221(57)
A (MHz)	4118.87378	4117.06130(41)
B (MHz)	2638.674317	2635.40528(43)
C (MHz)	2233.691145	2231.31624(28)
Δ_J (kHz)	0.448801	0.447169(92)
Δ_{JK} (kHz)	-0.444257	$-0.43483(30)$
Δ_K (kHz)	1.5875	1.58574(31)
δ_J (kHz)	0.109591	0.109331(60)
δ_K (kHz)	0.133538	0.13432(20)
Φ_J (Hz)	1.17×10^{-4}	$1.10(11) \times 10^{-4}$
Φ_{JK} (Hz)	-5.487×10^{-4}	$-5.80(37) \times 10^{-4}$
Φ_K (Hz)	2.17×10^{-3}	$2.329(47) \times 10^{-3}$
ϕ_J (mHz)	0.03935	0.0376(68)
ϕ_{JK} (mHz)	0.0818	0.0818[c]
ϕ_K (mHz)	-2.231	$-2.08(14)$
no. of lines		8739
max J, K_a, K_c		96, 68, 94
RMS error		0.00009 cm^{-1}

[a]Ground state constants taken from ref 11. [b]This work. Numbers in parentheses represent one standard deviation of the fitted value. [c]Fixed to ground state value.

number transitions assigned in the room temperature spectra. In contrast to ν_2, the ν_8 transitions show evidence of localized avoided crossings due to resonance perturbations. A preliminary "effective" fit to a single upper state revealed J-dependent crossings that occur in three distinct regions: around $K_a' = 23$, 34, and 70 with the last of these the most significant (Figure 3a). These perturbations were not uncovered in the earlier jet-cooled study as the quantum number range ($J' \leq 29$, $K_a' \leq 24$) was limited by the effective rotational temperature of 40 K.[22] The pattern of (obs − calc) residuals suggests interacting state(s) at lower wavenumber and the largest displacements around $K_a' = 70$ (which show $K_c' = 0$ lines being unaffected) appear consistent with a b-axis or c-axis Coriolis selection rule of $\Delta K_a = \pm 1$. Only one possible state in the right vicinity has the required B_1 or A_2 symmetry: $\nu_3 + \nu_4 + \nu_7$ (B_1) with an estimated position 1150 cm^{-1} ($\nu_3 + \nu_7$ is at 888.5 cm^{-1}, ν_4 at 261.6 cm^{-1}).[24]

A series of trial fits conducted with SPFIT[30] demonstrated that a vibrational state at 1150.2 cm^{-1} connected via a modest first-order b-axis Coriolis term $G_{8,347}^b$ (131 MHz) could satisfactorily account for the $K_a' \approx 70$ crossing and also for the smaller displacements around $K_a' \approx 34$ via the weaker $\Delta K_a = \Delta K_c = \pm 3$ interaction. In turn, the $\nu_3 + \nu_4 + \nu_7$ level is expected to be further connected to the nearby $\nu_3 + \nu_4 + \nu_9$ level: the MP2/aug-cc-PVTZ value for the dimensionless Coriolis parameter $\varsigma_{7,9}^b = -0.392$. It was found that this interaction could account for the $K_a' \approx 23$ crossing in ν_8 by indirect coupling with $\nu_3 + \nu_4 + \nu_9$ via $\nu_3 + \nu_4 + \nu_7$, resulting in a $\Delta K_a = \pm 2$ selection rule, as illustrated in Figure 3b. A comparable example of indirect Coriolis coupling was recently reported involving the $\nu_3 + \nu_4$ and $\nu_2 + 2\nu_4$ states of NO_3.[32] In the case of $CH^{35}ClF_2$ (R22), it was possible to confirm the Coriolis interaction of ν_3 with the "dark" $3\nu_9$ state by assignment of a small number of the most heavily mixed "dark" $3\nu_9$ state transitions.[33] In the present case, predictions from Pickett's SPCAT program[30] indicate that the most intense lines of the "dark" $\nu_3 + \nu_4 + \nu_9$ state (with intensities around 7%

Table 3. Spectroscopic Constants of the Ground State and the ν_2 and ν_8 Fundamental Bands of C^{35}Cl^{37}ClF$_2$

parameter	ground state[a]	$\nu_2 = 1$[a]	$\nu_8 = 1$[a]
ν_0 (cm^{-1})		667.207512(12)	1160.964899(9)
A (MHz)	4092.01667(52)	4090.31698(38)	4101.08465(70)
B (MHz)	2582.22356(50)	2579.07628(31)	2581.73120(114)
C (MHz)	2185.44422(49)	2183.17560(18)	2184.05711(87)
Δ_J (kHz)	0.432518(94)	0.430991(43)	0.43621(34)
Δ_{JK} (kHz)	$-0.437765(39)$	$-0.42781(19)$	$-0.3898(16)$
Δ_K (kHz)	1.585732(49)	1.58301(31)	1.7918(15)
δ_J (kHz)	0.105647(42)	0.105318(25)	0.10697(20)
δ_K (kHz)	0.14333(63)	0.14211(35)	0.1748(36)
Φ_J (Hz)	1.17×10^{-4}	1.17×10^{-4} [b]	1.17×10^{-4} [b]
Φ_{JK} (Hz)	-5.487×10^{-4}	-5.487×10^{-4} [b]	-5.487×10^{-4} [b]
Φ_K (Hz)	2.17×10^{-3}	$2.163(41) \times 10^{-3}$	$7.187(96) \times 10^{-3}$
ϕ_J (mHz)	0.03935	0.03935[b]	0.03935[b]
ϕ_{JK} (mHz)	0.0818	0.0818[b]	0.0818[b]
ϕ_K (mHz)	-2.231	-2.231[b]	-2.231[b]
no. of lines	87 MW, 3007 IR	5857	3893
max J, K_a, K_c	81, 65, 81	92, 71, 91	71, 67, 55
RMS error	0.00016 cm^{-1}, 0.038 MHz	0.00009 cm^{-1}	0.00014 cm^{-1}

[a]Each column contains data from a separate fit (see text), with numbers in parentheses being one standard deviation of the fitted value. The sextic constants were fixed to the values of the C^{35}Cl$_2$F$_2$ isotopologue. [b]Fixed to the ground state values.
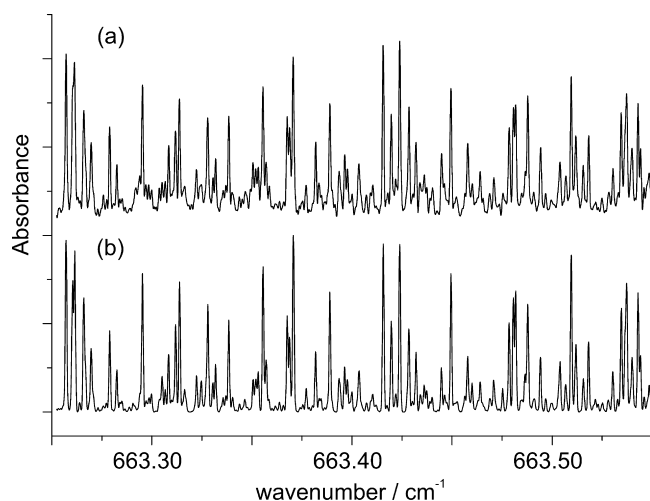

Figure 2. (a) Portion of the high-resolution infrared spectrum of ν_2 of R12. (b) Simulation of the same section of the spectrum using PGopher[29] with a rotational temperature of 155 K and a Gaussian line width of 0.000 90 cm^{-1}. Contributions from both C^{35}Cl$_2$F$_2$ and C^{35}Cl^{37}ClF$_2$ have been summed together. Any additional features not accounted for are from the C^{37}Cl$_2$F$_2$ isotopologue or hot bands.

Figure 3. (a) Obs − calc residuals vs quantum number index $K_a{}' + 0.01 \times J'$ from an "effective" one-state fit to ν_8 transitions of C^{35}Cl$_2$F$_2$ that does not account for resonance interactions. The three regions of avoided crossings around $K_a{}' = 23$, 34, and 70 are due to the indirect $\Delta K_a = 2$ interaction with $\nu_3 + \nu_4 + \nu_9$, and the direct $\Delta K_a = 3$ and $\Delta K_a = 1$ interactions with $\nu_3 + \nu_4 + \nu_9$, respectively. (b) Energy level schematic showing the Coriolis interactions responsible for local avoided crossings for the ν_8 of C^{35}Cl$_2$F$_2$.

of the strongest ν_8 line) are six pairs of degenerate P- and R-branch transitions that involve heavily mixed $J' = 34-36$, $K_a{}' = 25$ levels. All of these were observed with positions and intensities consistent with the prediction and they were subsequently included in the final least-squares fit. For $\nu_3 + \nu_4 + \nu_7$ and $\nu_3 + \nu_4 + \nu_9$, all but one centrifugal distortion constant were fixed to their corresponding ground state values. The inclusion of a second-order Coriolis interaction parameter $F_{7,9}^{ac}$ helped to lower the standard deviation of the fit. The success of this three-state treatment summarized in Table 4 is demonstrated by the low rms error of 0.000 18 cm^{-1} achieved for the ν_8 transitions and the fact that even in the perturbed region the residuals come down to ≤ 0.001 cm^{-1}. Further support for the physically realistic nature of the model is provided by comparison of the predicted $\nu_3 + \nu_4 + \nu_9$ band
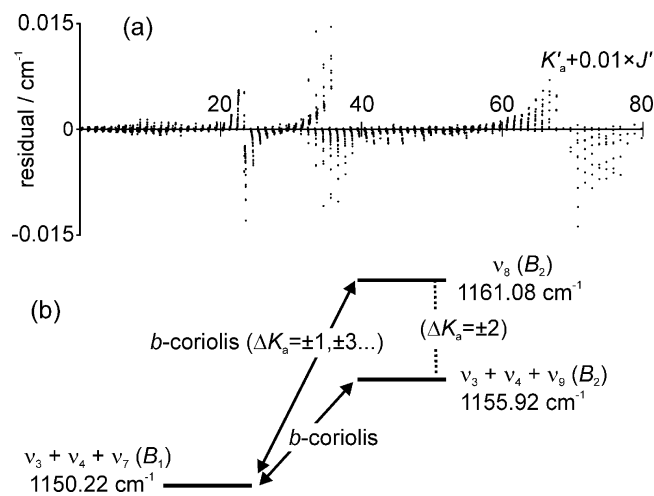
center of 1155.8 cm^{-1} [458.6 + 261.6 + 437.0 = 1157.2 cm^{-1}, adjusted to 1155.8 cm^{-1} by taking account the anharmonic constants $x_{3,4} = -0.7$, $x_{3,9} = -0.5$, and $x_{4,9} = -0.2$ at the CCSD(T)/cc-pVTZ level (from ref 34) or similarly $x_{3,4} = -0.6$, $x_{3,9} = -0.5$, and $x_{4,9} = -0.3$ at the MP2/aug-cc-PVTZ level] with the fitted value of 1155.92 cm^{-1}, and of the predicted first-order Coriolis parameter $G_{7,9}^{b}$ ($G_{7,9}^{b} \approx 2A\varsigma_{7,9}^{b} = 2067$ MHz) with 2180 MHz from the fit.

Analysis of ν_8 C^{35}Cl^{37}ClF$_2$. The C^{35}Cl^{37}ClF$_2$ isotopologue has a concentration 64% of that for C^{35}Cl$_2$F$_2$ at natural abundance. Although it was possible to assign transitions of C^{35}Cl^{37}ClF$_2$ by Loomis Wood analysis of the measured spectra, many of its lines are overlapped or obscured by the stronger C^{35}Cl$_2$F$_2$ component. Under these circumstances, it is desirable

2483

dx.doi.org/10.1021/jp501302q | J. Phys. Chem. A 2014, 118, 2480−2487

Table 4. Spectroscopic Constants of the Fundamental Band ν_8 of $C^{35}Cl_2F_2{}^a$

parameter	$\nu_8 = 1$	$\nu_3 = \nu_4 = \nu_7 = 1$	$\nu_3 = \nu_4 = \nu_9 = 1$
ν_0 (cm^{-1})	1161.085138(4)	1150.22092(58)	1155.92467(28)
A (MHz)	4128.069582(93)	4138.6264(128)	4109.9934(127)
B (MHz)	2638.209239(174)	2640.3796(215)	2626.9509(167)
C (MHz)	2232.251501(197)	2226.3251(219)	2223.4522(231)
Δ_J (kHz)	0.4488424(122)	0.448801^b	0.448801^b
Δ_{JK} (kHz)	−0.3890273(221)	−2.28920(302)	−0.444257^b
Δ_K (kHz)	1.7939070(276)	1.5875^b	1.5875^b
δ_J (kHz)	0.1091710(432)	0.109591^b	0.109591^b
δ_K (kHz)	0.170630(285)	0.133538^b	0.133538^b
Φ_J (Hz)	0.000117^b	0.000117^b	0.000117^b
Φ_{JK} (Hz)	0.00030370(371)	−0.000548^b	−0.000548^b
Φ_K (Hz)	0.00627260(553)	0.00217^b	0.00217^b
ϕ_J (mHz)	0.03935^b	0.03935^b	0.03935^b
ϕ_{JK} (mHz)	0.0818^b	0.0818^b	0.0818^b
ϕ_K (mHz)	−2.231^b	−2.231^b	−2.231^b
$G_{8,347}^{b}$ (MHz)^c	← 130.874(110) →		
$G_{7,9}^{b}$ (MHz)^c		← 2179.810(466) →	
$F_{7,9}^{ac}$ (MHz)^c		← −8.4838(112) →	
no. of lines	6180		12
max J, K_a, K_c	93, 80, 47		36, 25, 11
RMS error (cm^{-1})	0.00018		0.00127

^{a}Ground state constants taken from ref 11 in Table 2. Numbers in parentheses are one standard deviation of the fitted value. ^{b}Fixed to ground state value. ^{c}The first-order Coriolis interaction term is $iG_{7,9}^{b}P_b$, where $G_{7,9}^{b} = \varsigma_{7,9}^{b}B_e(\omega_7 + \omega_9)(\omega_7\omega_9)^{-1/2}$ and the second-order interaction is $F_{7,9}^{ac}(P_aP_c + P_cP_a)$.

to remove the interfering component if possible. When an isotopically pure experimental sample is unavailable, another method that has proven successful is to simulate the interfering band instead, a method we have called "spectral analysis by subtraction of simulated intensities (SASSI)".[35,36] This approach was employed in the analysis of ν_8: the $C^{35}Cl_2F_2$ component was simulated at 150 K and its subtraction from the corresponding cool spectrum revealed considerably more of the rovibrational structure due to $C^{35}Cl^{37}ClF_2$ (Figure 4). Almost 4000 lines were assigned and fitted to produce the molecular constants in the last column of Table 3, with an rms error of 0.000 14 cm^{-1}.

The residuals do not show evidence of the perturbations seen in $C^{35}Cl_2F_2$, probably due to isotopic shifts increasing the gap to the combinations levels. The ν_8 band is only 0.12 cm^{-1} lower, but $\nu_3 + \nu_4 + \nu_7$ is expected to shift −7.8 cm^{-1} ($\nu_3 + \nu_7$ shifts −5.3 cm^1 and ν_4 by −2.5 cm^1),[24] and similarly $\nu_3 + \nu_4 + \nu_9$ by −6.5 cm^{-1}. Thus the avoided crossings will occur at much higher $K_a{}'$ quantum number, and the indirect $\Delta K_a = \pm 2$ interaction will be considerably weakened by the greater separation to the relevant intermediate $\nu_3 + \nu_4 + \nu_7$ levels. The need to vary the sextic Φ_K parameter and its larger magnitude (7.19×10^{-3}) than the corresponding ground state constant (2.17×10^{-3}) does hint at a remaining untreated K_a-dependent perturbation, and one that similarly affects the $C^{35}Cl_2F_2$ constants in Table 4. The most feasible candidate is the a-axis Coriolis interaction with ν_1: the MP2/aug-cc-PVTZ value for the dimensionless Coriolis parameter $\varsigma_{1,8}^{a} = 0.770$.

The molecular parameters in Tables 3 and 4 can satisfactorily reproduce the line positions of the ν_8 fundamental transitions; see Figure 4, for example. However, inspection of the entire band profile reveals some differences between simulated and experimental traces (Figure 5). First, the experimental spectrum contains some additional weak lines due to $C^{37}Cl_2F_2$ (6% of the concentration in natural abundance) and to hot bands that are
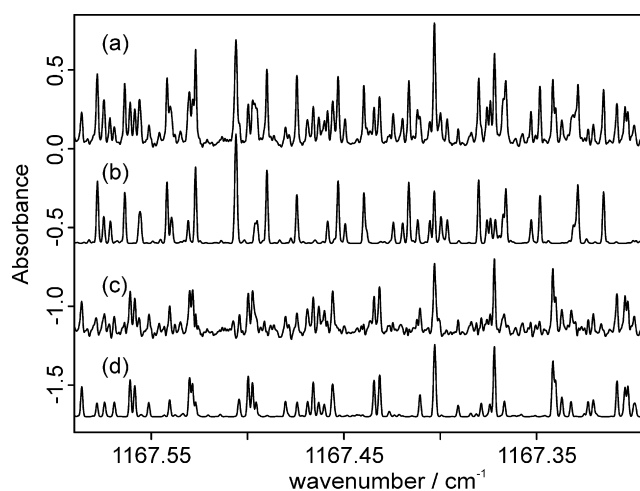

Figure 4. Comparison of (a) an expanded experimental spectrum of the ν_8 band, (b) a simulation of ν_8 for $C^{35}Cl_2F_2$ only, (c) the resultant, subtracted spectrum, and (d) a simulation of the $C^{35}Cl^{37}ClF_2$ component. For the simulations, line positions and intensities at $T = 150$ K were generated with Pickett's SPCAT program[30] and convolved using a Gaussian line shape with fwhm line width 0.0012 cm^{-1}.

evident even at 150 K from weak Q-branch heads seen a few wavenumbers lower than those of the fundamental. These additional lines contribute to the slightly raised baseline of the experimental spectrum. Second, the intensity distribution is not quite right for simulation I employing a conventional c-type dipole moment, μ_c, only. The experimental spectrum is stronger in the P-branch and weaker in the R-branch, an effect that increases with distance from the band center. The most likely cause is the yet untreated a-axis Coriolis interaction with ν_1 alluded to above. Large Coriolis parameters between nearby states can give rise to significant intensity variations. Bands with zero or very low inherent strength may become allowed via the
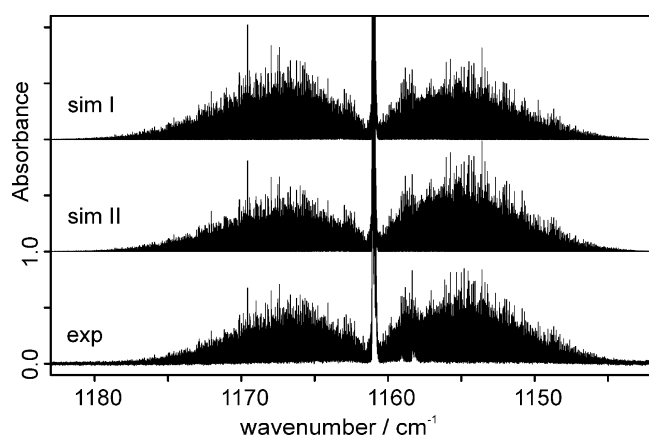
Figure 5. Experimental spectrum (2.0 Pa, 2.5 m path length) in the ν_8 region along with simulations at 150 K based on the ν_8 fundamentals of both $C^{35}Cl_2F_2$ and $C^{35}Cl^{37}ClF_2$. Simulation I is based on a conventional c-type dipole moment, μ_c. Simulation II adds to this a first-order Herman–Wallis correction $^1/_2[P^2,\phi_c]$ (in SPCAT[30] designated 50013 with empirically determined value of -0.12, included along with the regular 013 dipole with value 1.0).

Coriolis-induced mixing, e.g., $F_2C{=}CH_2$,[37] though the resultant profile will be quite atypical due to the quantum number dependence of the wave function mixing, as seen in ketenimine.[38,39] When both bands are allowed, what Mills describes as a "positive perturbation" leads to enhancement of the P-branch of the high-frequency band and the R-branch of the low-frequency band.[40] A preliminary simulation of Coriolis-coupled ν_1 and ν_8 improved the intensity profile considerably. Rigorous incorporation of the ν_1 state via a combined fit is no trivial undertaking because ν_1 itself is coupled to $\nu_3 + 2\nu_5$, $\nu_2 + \nu_3$, $\nu_2 + \nu_7$, and $\nu_2 + \nu_9$. This will be further elucidated in the work to be published on ν_1.[14] However, the effects of this a-axis Coriolis interaction may be approximated by adding an empirically determined Herman–Wallis correction term.[41] Simulation II of Figure 5 shows a much improved ratio of P/R branch transitions.

CONCLUSIONS

High-resolution infrared spectroscopy and rovibrational analysis of a molecule like R12 is particularly challenging due to spectral congestion and to the confounding effects of resonance perturbations. With regard to congestion, R12 has the complication of isotopologues associated with two chlorine atoms. Its relatively large size gives rise to small rotational constants thereby increasing the rotational partition function and the number of rovibrational transitions while narrowing the envelope within which they are found, and low-frequency vibrations also contribute to significant hot-band population. Assignment of transitions requires that they be sufficiently resolved, but at room temperature even the best available instrumental resolution (nominally 0.000 96 cm^{-1} here) is not sufficient. In the previous ν_8 study jet cooling to 40 K reduced the number of populated levels to the extent that a spectral resolution of 0.0034 cm^{-1} was sufficient for assignment, but the drawback was accessing only a limited range of rotational quantum numbers. In the present study a temperature of around 150 K is a happy medium between spectral resolution and the quantum number range of assignable transitions, though the wings of the room temperature spectrum can also be helpful for detecting some additional transitions with high

quantum numbers. When more than one spectral component is present, subtraction of one or more of these via their simulated spectra (SASSI) can also prove very useful, as illustrated by removal of the ν_8 $C^{35}Cl_2F_2$ lines to facilitate assignment of $C^{35}Cl^{37}ClF_2$ transitions described here.

Following the assignment of transitions, they must be fitted and the band satisfactorily modeled, which is where global and local resonance perturbations present another challenge. The low-frequency vibrational modes of R12 tend to increase the number of combination or overtone levels that are found in close proximity to a given band, which might therefore give rise to local interactions. For the most part these combination levels are "dark", i.e., with vanishingly small inherent transition strength, and the resonance interaction terms small so that they are manifest only through local avoided crossings in the observed bands. One strategy is to note these crossings but omit a subset of the transitions most affected. However, it is often possible to treat these resonances by including the "dark" states in the fit, as illustrated in the $C^{35}Cl_2F_2$ ν_8 case where even the indirect local perturbation with $\nu_3 + \nu_4 + \nu_9$, mediated via $\nu_3 + \nu_4 + \nu_7$ could be accounted for. Global perturbations involving significant Fermi or Coriolis resonance terms can affect the entire band. When the interacting states are far enough apart that the separation of levels has little quantum number dependence, effective parameters can account for the wavenumber shifts: Fermi resonances merely shift the band centers whereas Coriolis resonances change the relevant rotational constant in both states. In R12, however, ν_1 and ν_8 are close enough that in the absence of the K_a-dependent a-axis Coriolis interaction, an anomalously large sextic Φ_K parameter is needed for ν_8. More seriously, simulations show that the band intensity is not satisfactorily reproduced without explicit inclusion of the interaction or the introduction of Herman Wallis corrections. In the ν_2 case, it is fortunate there are no other vibrational levels within 25 cm^{-1} and so no local perturbations were observed. The fitted parameters are able to reproduce the observed spectrum to a high degree of accuracy, which would make the resulting parameters ideal for use in analyzing R12 in the atmosphere using infrared based satellite systems although there may be interference from the overlapping CO_2 band.

ASSOCIATED CONTENT

ⓈSupporting Information

The supplementary data contains fits of the upper states of $C^{35}Cl_2F_2$ and $C^{35}Cl^{37}ClF_2$ and the result of the ground state combination difference fit of $C^{35}Cl^{37}ClF_2$ including all the assigned transitions. This material is available free of charge via the Internet at http://pubs.acs.org.

AUTHOR INFORMATION

Corresponding Author
*E. G. Robertson: e-mail, e.robertson@latrobe.edu.au.

Present Address
⊥Max-Planck-Institut für Struktur und Dynamik der Materie, 22761 Hamburg, Germany.

Notes
The authors declare no competing financial interest.

ACKNOWLEDGMENTS

Quantum chemistry calculations were carried out using facilities at Australia's National Computational Infrastructure National Facility (NCI-NF).

■ REFERENCES

(1) Solomon, S.; Qin, D.; Manning, M.; Chen, Z.; Marquis, M.; Averyt, K. B.; Tignor, M.; Miller, H. L. *Contribution of Working Group I to the Fourth Assessment Report of the Intergovernmental Panel on Climate Change*; Cambridge University Press: Cambridge, U.K., and New York, NY, USA, 2007.

(2) Elkins, J. W.; Dutton, G. S. [Global Climate] Atmospheric Composition [in "State of the Climate in 2010"]. *B Am. Meteorol. Soc.* **2011**, *92*, S60−S61.

(3) Bera, P. P.; Francisco, J. S.; Lee, T. J. Identifying the Molecular Origin of Global Warming. *J. Phys. Chem. A* **2009**, *113*, 12694−12699.

(4) Prinn, R. G.; Weiss, R. F.; Fraser, P. J.; Simmonds, P. G.; Cunnold, D. M.; Alyea, F. N.; O'Doherty, S.; Salameh, P.; Miller, B. R.; Huang, J.; et al. A History of Chemically and Radiatively Important Gases in Air Deduced from ALE/GAGE/AGAGE. *J. Geophys. Res., [Atmos.]* **2000**, *105*, 17751−17792.

(5) Advanced Global Atmospheric Gases Experiment. http://agage. eas.gatech.edu/.

(6) Coheur, P. F.; Clerbaux, C.; Colin, R. Spectroscopic Measurements of Halocarbons and Hydrohalocarbons by Satellite-Borne Remote Sensors. *J. Geophys. Res., [Atmos.]* **2003**, *108*, 4130.

(7) Booker, R. A.; Delucia, F. C. The Millimeter-Wave Spectrum of CCl_2F_2. *J. Mol. Spectrosc.* **1986**, *118*, 548−549.

(8) Davis, R. W.; Gerry, M. C. L.; Marsden, C. J. The Microwave-Spectrum, Harmonic Force-Field, and Structure of Difluorodichloromethane. *J. Mol. Spectrosc.* **1983**, *101*, 167−179.

(9) Takeo, H.; Matsumura, C. Microwave-Spectrum of Dichlorodifluoromethane. *Bull. Chem. Soc. Jpn.* **1977**, *50*, 636−640.

(10) Su, C. F.; Beeson, E. L. Nuclear-Quadrupole Coupling Effects in Microwave-Spectrum of Dichlorodifluoromethane. *J. Chem. Phys.* **1977**, *66*, 330−334.

(11) Baskakov, O. I.; Dyubko, S. F.; Katrich, A. A.; Ilyushin, V. V.; Alekseev, E. A. Millimeter-Wave Spectrum of CCl_2F_2, Taking into Account the Hyperfine Structure. *J. Mol. Spectrosc.* **2000**, *199*, 26−33.

(12) Taubmann, G.; Jones, H. Double-Resonance Spectroscopy of Freon-12 - Hot Bands of $CF_2{}^{35}Cl_2$ and $CF_2{}^{35}Cl^{37}Cl$ and the v_6 Fundamental of $CF_2{}^{37}Cl_2$. *J. Mol. Spectrosc.* **1986**, *117*, 283−291.

(13) LeBlanc, L. M.; Anderson, A. Raman and Infrared-Spectra of the Solid Chlorofluorocarbons. II-Dichlorodifluoromethane. *J. Raman Spectrosc.* **1991**, *22*, 255−260.

(14) Robertson, E. G.; Medcraft, C.; McNaughton, D.; Appadoo, D. The Limits of Rovibrational Analysis: the Severely Entangled ν_1 Vibration of Dichlorodifluoromethane in the Greenhouse IR Window.- *Manuscript in preparation*.

(15) Giorgianni, S.; Gambi, A.; Franco, L.; Ghersetti, S. Infrared-Spectrum and Molecular-Force Field of CCl_2F_2. *J. Mol. Spectrosc.* **1979**, *75*, 389−405.

(16) Nordstrom, R. J.; Morillon-Chapey, M.; Deroche, J. C.; Jennings, D. E. First Study of the ν_6 Fundamental of CCl_2F_2. *J. Phys. Lett.-Paris* **1979**, *40*, L37−L40.

(17) Jones, H.; Morillon-Chapey, M. The 923 cm^{-1} Band of ($C^{35}Cl_2F_2$), Studied by Infrared Microwave Double-Resonance. *J. Mol. Spectrosc.* **1982**, *91*, 87−102.

(18) Jones, H.; Taubmann, G.; Morillon-Chapey, M. The ν_6 Band of $C^{35}Cl^{37}ClF_2$ from IR-MW Double-Resonance. *J. Mol. Spectrosc.* **1985**, *111*, 179−184.

(19) Meerts, W. L.; Snels, M. High-Resolution Spectroscopy of Dichlorodifluoromethane in a Molecular Jet. *Appl. Phys. B: Laser Opt.* **1988**, *B45*, 27−31.

(20) Giorgianni, S.; Gambi, A.; Baldacci, A.; Delorenzi, A.; Ghersetti, S. Infrared Study of the ν_1 Band of CCl_2F_2 by Diode-Laser Spectroscopy. *J. Mol. Spectrosc.* **1990**, *144*, 230−238.

(21) McNaughton, D.; McGilvery, D.; Robertson, E. G. High-Resolution FTIR Spectroscopy of CFCs in a Supersonic Jet Expansion. *J. Mol. Struct.* **1995**, *348*, 1−4.

(22) McNaughton, D.; McGilvery, D.; Robertson, E. G. High-Resolution FTIR Jet Spectroscopy of CCl_2F_2. *J. Chem. Soc., Faraday Trans.* **1994**, *90*, 1055−1060.

(23) McNaughton, D.; Robertson, E. G.; Thompson, C. D.; Chimdi, T.; Bane, M. K.; Appadoo, D. Overview of High-Resolution Infrared Measurement and Analysis for Atmospheric Monitoring of Halocarbons. *Anal. Chem.* **2010**, *82*, 7958−7964.

(24) D'Amico, G. D.; Snels, M.; Hollenstein, H.; Quack, M. Analysis of the $\nu_3+\nu_7$ Combination Band of CF_2Cl_2 from Spectra Obtained by High Resolution Diode Laser and FTIR Supersonic Jet Techniques. *Phys. Chem. Chem. Phys.* **2002**, *4*, 1531−1536.

(25) McKellar, A. R. W. High-resolution Infrared Spectroscopy with Synchrotron Sources. *J. Mol. Spectrosc.* **2010**, *262*, 1−10.

(26) Chimdi, T.; Robertson, E. G.; Puskar, L.; Thompson, C. D.; Tobin, M. J.; McNaughton, D. High Resolution Synchrotron FTIR Spectroscopy of the Far Infrared ν_{10} and ν_{11} Bands of R152a (CH_3CHF_2). *Chem. Phys. Lett.* **2008**, *465*, 203−206.

(27) Bauerecker, S.; Taraschewski, M.; Weitkamp, C.; Cammenga, H. K. Liquid-Helium Temperature Long-Path Infrared Spectroscopy of Molecular Clusters and Supercooled Molecules. *Rev. Sci. Instrum.* **2001**, *72*, 3946−3955.

(28) McNaughton, D.; McGilvery, D.; Shanks, F. High-Resolution FTIR Analysis of the ν_1 Band of Tricarbon Monoxide - Production of Tricarbon Monoxide and Chloroacetylenes by Pyrolysis of Fumaroyl Dichloride. *J. Mol. Spectrosc.* **1991**, *149*, 458−473.

(29) Western, C. M. *PGOPHER A Program for Simulating Rotational Structure, Version 7.1.108*; University of Bristol, 2010; http://pgopher. chm.bris.ac.uk.

(30) Pickett, H. M. The Fitting and Prediction of Vibration-Rotation Spectra with Spin Interactions. *J. Mol. Spectrosc.* **1991**, *148*, 371−377.

(31) Watson, J. K. G. In *Vibrational Spectra and Structure: A Series of Advances*; Durig, J. R., Ed.; Elsevier: Amsterdam, Oxford, 1977; Vol. 6.

(32) Kawaguchi, K.; Fujimori, R.; Tang, J.; Ishiwata, T. FTIR Spectroscopy of NO_3: Perturbation Analysis of the $\nu_3+\nu_4$ State. *J. Phys. Chem. A* **2013**, *117*, 13732−13742.

(33) Thompson, C. D.; Robertson, E. G.; McNaughton, D. Completing the Picture in the Rovibrational Analysis of Chlorodifluoromethane (CHClF$_2$): ν_3 and ν_8. *Mol. Phys.* **2004**, *102*, 1687−1695.

(34) Csontos, J.; Rolik, Z.; Das, S.; Kallay, M. High-Accuracy Thermochemistry of Atmospherically Important Fluorinated and Chlorinated Methane Derivatives. *J. Phys. Chem. A* **2010**, *114*, 13093−13103.

(35) Thompson, C. D.; Robertson, E. G.; McNaughton, D. Reading Between the Lines: Exposing Underlying Features of High Resolution Infrared Spectra (CHClF$_2$). *Phys. Chem. Chem. Phys.* **2003**, *5*, 1996−2000.

(36) Robertson, E. G.; McNaughton, D. Maximising Rovibrational Assignments in the ν_1 Band of NSCl by Spectral Analysis by Subtraction of Simulated Intensities (SASSI). *J. Mol. Spectrosc.* **2006**, *238*, 56−63.

(37) McKean, D. C.; van der Veken, B.; Herrebout, W.; Law, M. M.; Brenner, M. J.; Nemchick, D. J.; Craig, N. C. Infrared Spectra of $^{12}CF_2={}^{12}CH_2$ and $^{12}CF_2={}^{13}CH_2$: Quantum-Chemical Calculations of Anharmonicity, and Analyses of Resonances. *J. Phys. Chem. A* **2010**, *114*, 5728−5742.

(38) Bane, M. K.; Robertson, E. G.; Thompson, C. D.; Appadoo, D. R. T.; McNaughton, D. High-Resolution Fourier-Transform Infrared Spectroscopy of the ν_6 and Coriolis Perturbation Allowed ν_{10} Modes of Ketenimine. *J. Chem. Phys.* **2011**, *135*, 224306.

(39) Bane, M. K.; Thompson, C. D.; Robertson, E. G.; Appadoo, D. R. T.; McNaughton, D. High-Resolution FTIR Spectroscopy of the ν_8 and Coriolis Perturbation Allowed ν_{12} Bands of Ketenimine. *Phys. Chem. Chem. Phys.* **2011**, *13*, 6793−6798.

(40) Mills, I. M. Coriolis Interactions, Intensity Perturbations and Potential Functions in Polyatomic Molecules. *Pure Appl. Chem.* **1965**, *11*, 325−344.

(41) Braslawsky, J.; Ben-Areh, Y. First Order Intensity Perturbations for the Vibration-Rotation Lines of Asymmetric Rotor: Theory and Application. *J. Chem. Phys.* **1969**, *51*, 2233−2241.

2487

dx.doi.org/10.1021/jp501302q | *J. Phys. Chem. A* 2014, 118, 2480−2487